

Effect of Alloying on the Fermi Surface of Copper

L.-F. CHOLLET* AND I. M. TEMPLETON

National Research Council, Ottawa, Canada

(Received 29 January 1968)

The variation of $\langle 111 \rangle$ neck cross section and of $\langle 111 \rangle$ belly/neck ratio with alloy concentration have been measured in a number of rather dilute ($<0.1\%$) alloys of zinc, cadmium, aluminum, nickel, and palladium in copper. The scattering (Dingle) temperatures for neck and belly oscillations in these alloys have also been measured. The results for the nontransitional additives show good agreement with a rigid-band, simple heterovalent scatterer model. The results for a single palladium alloy were inconclusive, but those for the nickel alloys are best interpreted on the basis of Friedel's "virtual bound level" model, with about 0.4 electrons per nickel atom left in the conduction band. The "effective scattering temperature" of nickel for neck electrons in copper is found to be appreciably lower than that for belly electrons, in contrast with the approximate 1.5:1 ratio found for the nontransitional impurities.

I. INTRODUCTION

THE substitution of solute atoms into the crystal lattice of a solvent metal will affect the Fermi surface (FS) of the solvent and the behavior of electrons on it in a number of ways. If the valency of the solute atom is larger (or smaller) than that of the solvent, the FS will increase (or decrease) in volume and will inevitably suffer some change of shape. Changes of lattice constant on alloying can also change both the volume and the shape of the FS. Even when there is no valency difference or significant change of lattice constant (as, for instance, in an alloy between silver and gold), the change of electronic band structure that accompanies alloying will change the shape of the FS to at least a small extent. Electron-scattering effects will depend on the degree of physical and electronic disturbance to the periodicity of the lattice. Those electrons with s -type wave functions (e.g., most of those on the "belly" of the FS in a noble metal) will in general be scattered by any disturbance centred on an atom site, while those with p character (e.g., the noble metal "neck" electrons) will generally be scattered only when the disturbance spreads out appreciably into the interatomic region.

Of the various possible methods of studying the shape of the FS, those depending on low-temperature quantum effects [e.g., the de Haas-van Alphen (dHvA) effect] will, in any alloy studies, necessarily suffer from loss of signal amplitude due to the electron-scattering effects already mentioned. The alloy range which can be studied is then limited to below $\sim 1\%$ even for homovalent solutes. Among other possible techniques, positron annihilation offers some promise. Its lack of precision may well be outweighed by the absence of any limitation on the alloy concentration. These techniques have been discussed by Chambers.¹

A previous study of the dHvA effect in dilute noble-metal alloys,² using the pulsed-magnetic-field method, dealt in some detail with the question of relaxation

times of different groups of electrons, but covered only peripherally the effect of alloying on the size and shape of the FS. Other recent studies include those of Higgins and Marcus³ on the effect of alloying on the FS of zinc, using the dHvA effect observed by the torque method. The present experiments were intended primarily to study the effect of alloying on the FS of copper, examining particularly the neck cross section as having the greatest sensitivity to changes of FS volume and of band structure; however, some useful information about electron-scattering effects was also obtained. It will be convenient to deal with these two aspects of the work separately, following some discussion of the alloys and experimental equipment used.

II. EXPERIMENTS

A. Alloys

The alloy single crystals were prepared by slow cooling of a melt in a purified graphite crucible. The samples were spark-machined as $\langle 111 \rangle$ rods some 1.6 mm square and then spark-cut into lengths rather over 3 mm long. The orientation before, during, and after cutting was checked at each stage by taking back-reflection Laue pictures, so that in general samples were well within 1° of $\langle 111 \rangle$. The use of a Polaroid XR-7 attachment for the x-ray camera was a great help in this procedure. After cutting, the samples were carefully etched to be a close fit when cold in the 2-mm i.d. sample holder (see below). The residual resistivity of the alloys was measured both on a separate longer rod and, after running, on individual samples, using a spring-loaded four-contact holder. Generally, close correspondence was found between the nominal solute content and the residual resistance ratios when compared with figures for scattering cross section given by Linde⁴ and others. However, in the case of zinc as solute, the *apparent* zinc content was appreciably higher than had been added in preparation. Samples cut from both ends of the 0.1% alloy ingot showed

* National Research Council of Canada Postdoctorate Fellow. Present address: Laboratoire Suisse de Recherches Horlogères, Neuchâtel, Switzerland.

¹ R. G. Chambers (to be published).

² P. E. King-Smith, *Phil. Mag.* **12**, 1123 (1965).

³ R. J. Higgins and J. A. Marcus, *Phys. Rev.* **141**, 553 (1966).

⁴ J. O. Linde, 1939 thesis data in F. J. Blatt, *Solid State Phys.* **4**, 318 (1957).

TABLE I. Details of alloys and experimental results. The first number for each alloy refers to an ingot, the second to an individual specimen. The asterisks denote those figures for the zinc alloys which have been modified as explained in the text. Data on scattering cross sections of the various solutes in copper were obtained as follows: Cd, Al, Ni, Pd: Linde, *via* Blatt^a; Zn: Henry and Schroeder,^b also Dugdale^c; Cd: Lucke^d; Al: Weinberg^e; Ni: Schroeder *et al.*^f

Specimen	Nominal at. %	at. % from Resistivity	$(R_{RT} - R_{He})/R_{He}$	Resistivity ($10^{-8} \Omega \text{ cm}$)	$\Delta N/N$ (%)	F_N (10^7 G)	F_B/F_N	x_N ($^{\circ}\text{K}$)	x_B ($^{\circ}\text{K}$)
Cu 1/4						2.1744	26.722	0.87	
Cu 1/5						2.1744	26.716	0.72	
Cu 1/6	0.000	0.000	3000	0.06	0.000	2.1739	26.716	0.78	
Cu 1/7						2.1728	26.720	0.67	0.20
Cu 1/8						2.1744	26.724	0.62	0.37
CuZn 1/1		0.033*	144	0.83*	0.033	2.1787	26.657	2.3	
CuZn 1/2		0.033*	142	0.84*	0.033	2.1780	26.671	1.4	
CuZn 1/3	0.050	0.032*	149	0.80*	0.032	2.1794	26.661	1.4	
CuZn 1/4		0.036*	134	0.89*	0.036	2.1777	26.676	2.0	
CuZn 1/5		0.040*	119	1.00*	0.040	2.1782	26.672	1.5	
CuZn 2/1		0.099*	49	2.44*	0.099	2.1845		2.2	
CuZn 2/2	0.100	0.096*	50	2.40*	0.096	2.1833	26.609	2.4	
CuZn 2/3		0.104*	46	2.60*	0.104	2.1844	26.608	2.4	1.7
CuZn 2/4		0.106*	45	2.66*	0.106	2.1874	26.602	2.7	2.3
CuZn 3/1		0.064*	74	1.61*	0.064	2.1823	26.630	2.6	1.3
CuZn 3/2	0.080	0.059*	87	1.37*	0.059	2.1819		3.1	0.90
CuZn 3/3		0.068*	70	1.70*	0.068	2.1825	26.630	3.2	2.2
CuCd 4/2		0.042	133	1.27	0.042	2.1790	26.657	2.1	
CuCd 4/3		0.041	137	1.23	0.041	2.1789	26.652	1.1	
CuCd 4/4	0.050	0.041	139	1.21	0.041	2.1771	26.669	1.6	
CuCd 4/5		0.045	125	1.35	0.045	2.1772	26.668	1.6	
CuCd 4/6		0.044	129	1.31	0.044	2.1787	26.661	1.6	0.96
CuAl 3/3		0.012	111	1.52	0.024	2.1795	26.675	1.9	
CuAl 3/4	0.010	0.011	125	1.35	0.022	2.1770	26.687	1.6	
CuAl 3/5		0.011	128	1.32	0.022	2.1767	26.683	1.7	
CuAl 3/6		0.017	83	2.04	0.033	2.1783	26.670	2.2	
CuAl 5/1		0.019	73	2.32	0.038	2.1795	26.666	2.0	1.4
CuAl 5/2	0.020	0.020	70	2.42	0.040	2.1813	26.646	2.1	1.4
CuAl 5/3		0.018	74	2.28	0.037	2.1786	26.672	2.1	1.4
CuPd 1/1		0.029	65	2.60	-0.029	2.1738	26.717	1.6	
CuPd 1/2	0.020	0.037	52	3.24	-0.037	2.1752	26.705	1.7	1.6
CuPd 1/3		0.037	54	3.12	-0.037	2.1727	26.717	1.5	1.1
CuNi 2/1		0.011	115	1.53	-0.011	2.1753	26.707	1.3	0.84
CuNi 2/2	0.010	0.010	126	1.34	-0.010	2.1742	26.724	1.3	
CuNi 2/3		0.010	127	1.33	-0.010	2.1738	26.719	0.94	0.50
CuNi 2/4		0.011	120	1.41	-0.011	2.1737	26.727	1.3	1.0
CuNi 3/1		0.019	67	2.52	-0.019	2.1738	26.712	1.02	1.04
CuNi 3/2	0.020	0.019	67	2.52	-0.019	2.1734	26.735	1.0	
CuNi 3/3		0.022	61	2.76	-0.022	2.1738	26.736	0.96	1.08
CuNi 4/1		0.038	34	4.96	-0.038	2.1728	26.732	0.85	1.5
CuNi 4/2	0.040	0.037	35	4.82	-0.037	2.1716	26.760	1.2	1.9
CuNi 4/3		0.037	35	4.82	-0.037	2.1736	26.724	1.08	1.4
CuNi 4/4		0.041	32	5.27	-0.041	2.1706	26.743	1.02	1.6
CuNi 5/1		0.061	21	7.88	-0.061	2.1698		1.7	
CuNi 5/2	0.060	0.058	22	7.52	-0.058	2.1698		1.9	
CuNi 5/3		0.054	24	6.97	-0.054	2.1687		1.8	
CuNi 8/1						2.1697			
CuNi 8/2	0.080	0.061	21	8.05	-0.061	2.1703			
CuNi 8/3						2.1686			

^a See Ref. 4.

^b W. G. Henry and P. A. Schroeder, *Can. J. Phys.* **41**, 1076 (1963).

^c J. S. Dugdale, (private communication).

^d W. H. Lucke, *J. Appl. Phys.* **37**, 842 (1966).

^e I. Weinberg, *Phys. Rev.* **138**, 838 (1965).

^f See Ref. 27.

essentially the same resistivity, thus ruling out segregation as the cause of the discrepancy. Unfortunately, in this concentration range quantitative analysis is rather difficult—the concentration is rather high for spectrographic analysis and rather low for chemical analysis. However, several spectrographic analyses made by courtesy of D. S. Russell of our Division of Applied Chemistry confirmed very closely the *nominal* content of the 0.1% zinc alloy, and suggested some solute loss

during preparation of the two more dilute alloys. We have therefore drawn the conclusion that a small iron content (analyzed as about 1 ppm) was probably responsible for the observed discrepancies, and have taken the *analyzed* atomic percentages of zinc as giving the correct mean values for zinc content of the three copper-zinc ingots. The zinc content of individual samples cut from these ingots was then assumed to vary according to their resistance ratios.

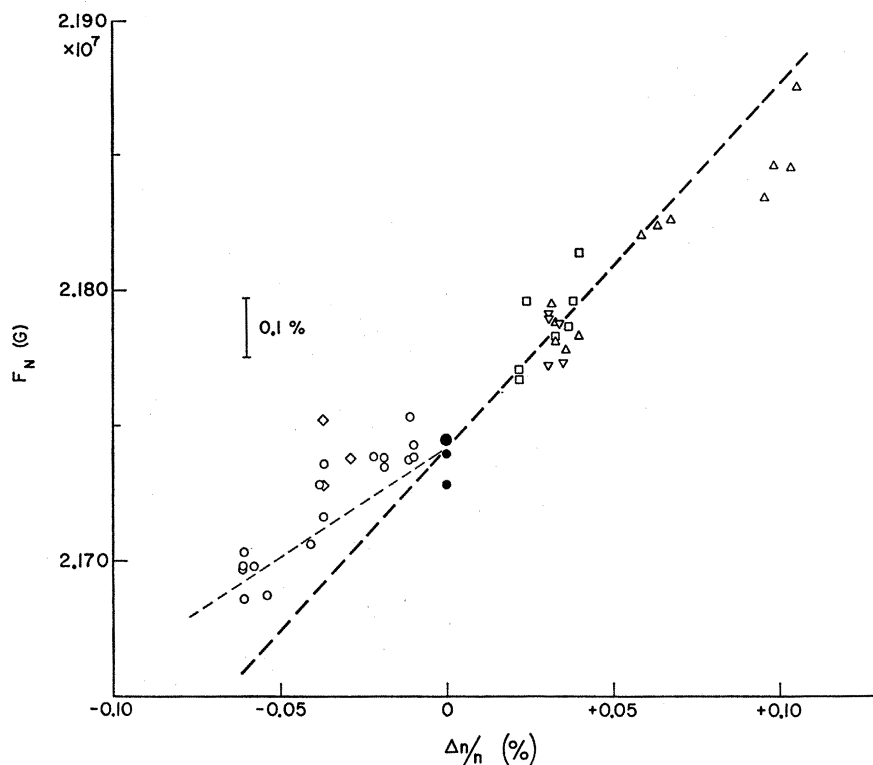


FIG. 1. Variation of neck dHvA frequency in copper with change of electron-to-atom ratio. Nickel and palladium treated as having zero valency. ●, pure copper; Δ, zinc alloys; ▽, cadmium alloys; □, aluminum alloys; ◇, palladium alloys; ○, nickel alloys. The heavy dashed line represents the rigid band prediction derived in the text.

Details of all the alloys are given in Table I. Those figures for the zinc alloys which have been modified to correspond with analysis are marked with an asterisk.

B. Experimental Equipment

The equipment used was essentially that employed in the study of the effect of hydrostatic pressure on the FS's of the noble metals.⁵ The samples were mounted in a fixed set of modulation and pickup coils in a beryllium copper "bomb." This has the advantage that the specimen is immersed in liquid helium condensed from an independent closed circuit, free from any possible contamination with solid air which can be a source of noise in some circumstances. This is particularly important in these experiments in view of the very small signal levels from the more concentrated alloys. The design of the equipment allows no significant movement of the sample relative to the magnetic field. It is, of course, important that the specimen be a close fit in the holder when cold. It is also important that the specimens be cut as near as possible to $\langle 111 \rangle$ to maximize signal and to minimize both the correction term required and any small errors due to remanent movement between sample and field. The sample in its bomb container was held axially in the tail of a pumped liquid helium Dewar vessel in the center of a 1-in.-i.d. superconducting solenoid. The dHvA oscillations were observed by a field-modulation technique, the modu-

lation and detection frequencies being 5 and 10 kc/sec, respectively.

C. Frequency and Frequency Ratio Measurements

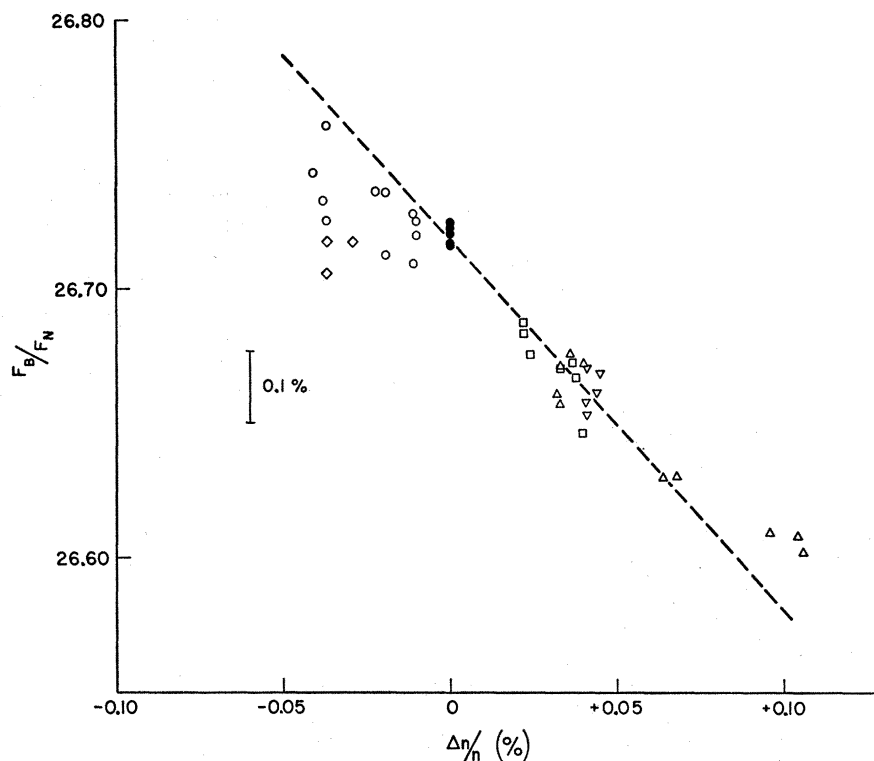
Neck Frequency

The magnetic-field range used for the neck-frequency measurements had to be sufficiently large to allow a precision of measurement appreciably better than 0.1% to be realized. In order to maintain equally high relative accuracy the range used had to be the same, or almost the same, for all the alloys measured. The upper limit was set by the amount of harmonic distortion⁶ which could be tolerated in the signals from the pure copper specimens which were measured to provide a reference frequency for the experiments, and the lower by the disappearance of signal in the more concentrated alloys. A suitable range, covering some 500 neck oscillations, was about 20 to 33 kG. This range was generally used except in the cases of a few of the most concentrated alloys, where the lower limit had to be raised to 23 kG. With the field-modulation level set to give maximum signal at the low end of the range, the magnetic field was swept slowly at about 50 G/sec. The oscillations, occurring initially at some 2.5 cps, were recorded against solenoid current on an x - y recorder and were also electronically counted. At every tenth

⁶ It was later realized that this distortion problem could have been avoided by making the reference measurements at an appreciably higher temperature than the 1°K used for the alloys.

⁵ I. M. Templeton, Proc. Roy. Soc. (London) A292, 413 (1966).

FIG. 2. Variation of belly/neck frequency ratio with change of electron-to-atom ratio. Details and symbols as in Fig. 1.



count a command pulse was automatically given to a Hewlett-Packard 3440A digital voltmeter to read the potential across a 0.1- Ω air-cooled manganin strip resistor in series with the superconducting solenoid. For most of the experiments these figures were printed out by a Hewlett-Packard 562A digital recorder and were later copied manually onto computer cards. In the final experiments, however, the figures were punched directly onto computer cards via a suitable interface unit and an IBM 526 punch. Several runs with increasing and decreasing fields were made on each specimen, giving about 50 data points per run. These figures were processed by computer using a simple program to give a least-squares linear fit to reciprocal magnetic field values. The program was also designed to test for false counts such as might occur with the noisy or low-level signals from the concentrated alloys, and mispunching during the manual copying process, by checking that any one reciprocal field interval lay within 5% of the mean interval. The slope (dHvA frequency) and probable error of the least-squares fit was printed out for each run. After taking the mean of up- and down-sweep results (which themselves only differed by a few tenths of 1%) the values obtained were consistent within a run to a few hundredths of a percent, and from run to run to at least 0.1%.⁷

⁷ The absolute value of the dHvA frequencies is believed to be correct to $\pm 0.1\%$, though this is not important for the present experiments. The calibration procedure for absolute measurements is described by Jan and Templeton (Ref. 18).

The observed neck frequencies had to be corrected for any known misorientation of sample, using the angular variation data of Joseph *et al.*,⁸ and for change of lattice constant on alloying, using the (room-temperature⁹) alloy data collected by Pearson¹⁰ and the hydrostatic pressure results of Templeton.⁵ These corrections were generally small, the largest lattice constant corrections being for the cadmium and palladium alloys. For the worst misorientation, of about 1.5°, the correction in F was only 0.1%, and any error arising from a mounting uncertainty of perhaps 0.2° would even in this case be within the experimental error in measuring F . The corrected neck frequencies are listed in Table I and shown in Fig. 1.

Belly/Neck Frequency Ratio

The relatively large change of the neck cross section on alloying may also be examined, under suitable conditions, in terms of the change in the belly/neck frequency ratio. The fractional change of this ratio will simply be the difference between those of the individual belly and neck frequencies, i.e.,

$$d \ln(F_B/F_N) = d \ln F_B - d \ln F_N. \quad (1)$$

⁸ A. S. Joseph, A. C. Thorsen, E. Gertner, and L. E. Valby, Phys. Rev. **148**, 569 (1966).

⁹ No allowance was made for the variation of this change with temperature.

¹⁰ W. B. Pearson, *Handbook of Lattice Spacings and Structures of Metals* (Pergamon Press, Inc., New York, 1958).

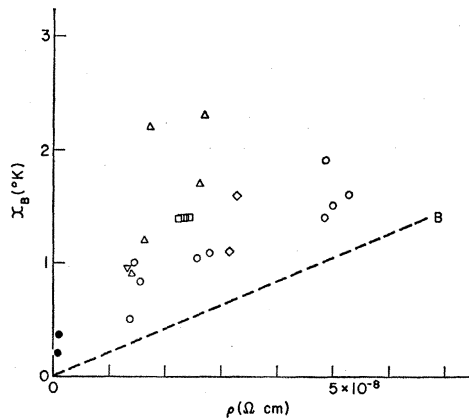


FIG. 3. Scattering temperature for belly electrons as a function of alloy resistivity. The dashed line B represents the lower limit derived by Brailsford (see text). Symbols as in Fig. 1.

In this way the belly cycles act as an internal reference scale, eliminating some potential sources of error. Unfortunately, the belly oscillations are more sensitive to impurity scattering than are the neck oscillations, so this technique is restricted to an even smaller range of alloy concentration than is the direct measurement of neck frequency. Some useful measurements were possible, however. The magnetic field was increased to a level such that, with appropriate modulation, combined neck and belly oscillations could be observed. These were recorded over about 30 neck cycles, and the frequency ratio was then determined by counting the number of neck and belly cycles between limits at which some recognizable form of phase coincidence occurred.

These results again had to be corrected for angular errors and lattice constant changes using data from the same sources as before. They are listed in Table I and shown in Fig. 2.

D. Scattering Temperature Measurements

Introduction

The parameter α , or "scattering temperature"¹¹ for electrons in a dHvA orbit can be derived from a knowledge of the cyclotron mass and the variation of signal amplitude with magnetic field (see, e.g., Ref. 2). Some measurements of scattering temperature were made during these experiments, but only to a secondary extent. It has since become clear that truly quantitative results can only be obtained under somewhat ideal conditions which were not generally fulfilled during this work. However, the results obtained do perhaps still have some qualitative value.

The difficulties involved are various. *Skin depth* is a factor that must be considered. Since the measurements were made at 10 kc/sec the skin depth in zero field in the purest samples was probably as small as 10^{-2} mm.

¹¹ R. B. Dingle, Proc. Roy. Soc. (London) A211, 517 (1962).

The skin depth in the more concentrated alloys was appreciably greater; however, a study of magneto-resistance data (see, e.g., Klauder *et al.*¹²) suggests that with the magnetic field along $\langle 111 \rangle$ we might expect in all samples a skin depth of some 10^{-1} mm at the middle of the range of magnetic field used in the measurements. The magnetoresistance in this range will probably be varying roughly linearly with field,¹³ so the skin depth will vary as $H^{1/2}$. Such a variation will cause a spurious increase of signal amplitude with field, resulting in a small increase in the calculated value of α (about 0.1°K for belly and 0.2°K for neck measurements). A further possibility is the presence of a small amount of remanent spark-cutting damage which decreases with depth into the sample. Any magnetoresistive increase of skin depth can then produce an additional increase of signal

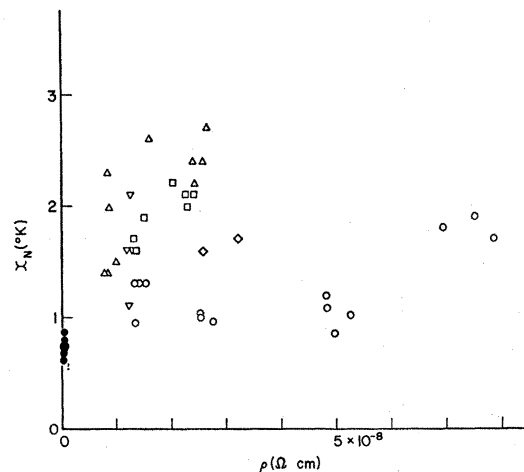


FIG. 4. Scattering temperature for neck electrons as a function of alloy resistivity. Symbols as in Fig. 1.

strength with magnetic field as less damaged material becomes involved as a source of signal. These problems may, in principle, be avoided by making the measuring frequency sufficiently low that the skin depth becomes large compared with the sample dimensions, but this argues a measuring frequency in the tens of cycles per second with attendant deterioration of signal-to-noise ratio.

A further, though probably less serious problem still remains. Because of interaction effects the magnetization oscillations at the higher fields in the purer materials may no longer be even approximately sinusoidal. Even if the modulation level is optimized at all fields (i.e., maximizing the second harmonic signal and keeping the modulation level proportional to the square of the magnetic field) the resulting signal may still not give the intended measure of amplitude versus

¹² J. R. Klauder, W. A. Reed, G. F. Brennert, and J. E. Kunzler, Phys. Rev. 141, 592 (1966).

¹³ W. A. Reed (private communication) confirms that the variation is closely linear over a relatively wide field range.

magnetic field. If the measurements are made, as they were in the case of the neck oscillations, with *constant* modulation amplitude, then the effect of harmonic distortion at the higher fields may be rather more serious.

Measurements

Despite these complications some reasonable figures for x_N (neck) and x_B (belly) were obtained. The appropriate part of the Lifshitz-Kosevich¹⁴ formula for the amplitude of the magnetization oscillation in the dHvA effect is of the approximate form

$$M \propto H^{-1/2} \exp[-2\pi^2 mck(T+x)/ehH], \quad (2)$$

which may be rewritten

$$M \propto H^{-1/2} \exp[-K_0 m(T+x)/m_0 H], \quad (3)$$

where $K_0 = 146.9$ kG/°K.

If the modulation level in the present experimental technique is maintained constant then the observed signal amplitude must be corrected according to an experimentally determined amplitude/modulation relationship. This was done for the measurements on the neck oscillations, the amplitudes being taken directly from the recordings of signal against solenoid current. For the belly oscillations the modulation level was adjusted to be a constant fraction of a period (i.e., $\propto H^2$) at each field value for which the signal amplitude was measured. If we assume the variation of skin depth as $H^{1/2}$ as discussed above we require only to plot \log (amplitude) against H^{-1} to obtain a straight line from the slope of which, with knowledge of the effective mass for the orbit concerned and the absolute temperature, we obtain the value of x . This approach gave

satisfactorily linear plots for both neck and belly oscillations. It seems reasonable to suppose, then, that no very gross absolute errors were involved and that the relative values of x , at least, should have some significance. The results are listed in Table I and shown in Figs. 3–5.

III. RESULTS AND DISCUSSION

A. Fermi-Surface Effects

Heine¹⁵ has discussed the predictions of the rigid-band model and of possible departures from a rigid-band condition. We may simplify his approach for our particular case as follows¹⁶:

The rate of change of neck cross section with electron-to-atom ratio is given by the dimensionless quantity

$$S = (\Delta A/A)/(\Delta n/n), \quad (4)$$

where A is the neck area, n is the number of electrons per unit volume in pure copper, and ΔA is the change in area corresponding to a change Δn in the electron density due to alloying. If ΔA is corrected for the change in lattice spacing, and if Δn is referred to the unit volume of pure copper, the corresponding change ΔE of the Fermi energy E_F in the rigid-band model then satisfies the relationships

$$m_c = (\hbar^2/2\pi)(\Delta A/\Delta E), \quad (5)$$

$$N(E_F) = (\Delta n/\Delta E). \quad (6)$$

$N(E_F)$ is the density of states of pure copper at the Fermi level and m_c is the cyclotron mass at the necks. The density of states is related to the electronic specific heat by

$$N(E_F) = (m_t/\pi^4/3\hbar^2)(3n)^{1/3}, \quad (7)$$

where m_t is the thermal effective mass. If we combine these equations, and introduce the de Haas-van Alphen neck frequency of copper $F_N = A\hbar c/2\pi e$, we obtain

$$S = (16\pi^4/3)^{1/3}(\hbar c/e)(a^2 F_N)^{-1}(m_c/m_t), \quad (8)$$

where a is the lattice parameter of copper, related to the electron density by $n = 4/a^3$.

S can be calculated from experimental data, namely, $a = 3.603 \times 10^{-8}$ cm,¹⁷ $F_N = 2.174 \times 10^7$ G,¹⁸ $m_c = 0.46m_e$,⁸ and $m_t = 1.39m_e$,¹⁹ giving $S = 6.2$, which determines the slope of the heavy dashed line in Fig. 1. It is interesting to note that the values of m_c and m_t predicted by the eight-cone model of Ziman²⁰ lead to $S = 12$. To calculate the fractional change of *belly* cross section on alloying we simply use the appropriate values of $F_B (= 5.809$

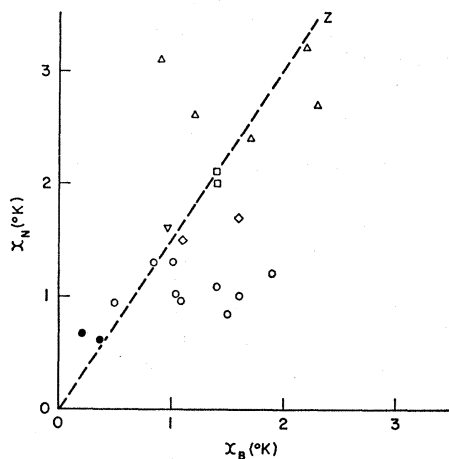


FIG. 5. Scattering temperature of neck electrons as a function of the scattering temperature for belly electrons in the same alloy. The dashed line Z represents Ziman's derivation of $x_N/x_B \approx 1.5$ for heterovalent scatterers. Symbols as in Fig. 1.

¹⁴ I. M. Lifshitz and A. M. Kosevich, Zh. Eksperim. i Teor. Fiz. 29, 730 (1955) [English transl.: Soviet Phys.-JETP 2, 636 (1956)].

¹⁵ V. Heine, Proc. Phys. Soc. (London) A69, 505 (1956).

¹⁶ We are indebted to Dr. J.-P. Jan for this derivation.

¹⁷ As used by D. Shoenberg, Phil. Trans. Roy. Soc. London A255, 85 (1962).

¹⁸ J.-P. Jan and I. M. Templeton, Phys. Rev. 161, 556 (1967).

¹⁹ D. L. Martin, Phys. Rev. 141, 576 (1966).

²⁰ J. M. Ziman, Advan. Phys. 10, 1 (1961).

$\times 10^8$ G) and m_c ($=1.36m_e$), taken from the same experimental sources. The value obtained for S is then 0.69, which is very close to the value of $\frac{2}{3}$ expected for a spherical Fermi surface. The rate of change of belly/neck frequency ratio with electron-to-atom ratio should then be about $0.7-6.2 = -5.5$, which is the value used for the dashed line in Fig. 2.

The results on neck cross section shown in Fig. 1, which are essentially repeated with some reduction of alloy range in the belly-to-neck ratios shown in Fig. 2, seem to be in remarkably good agreement with the semitheoretical results derived above as far as the higher valency additives are concerned. The slight fall off in the 0.1% zinc alloy might be interpreted as being due to a slight increase in the density of states at the new Fermi level. This result is well supported by the x-ray K -absorption measurements of Yeh and Azaroff²¹ who report results on copper-zinc in good agreement with a shared s -band rigid-band model. The situation is quite different for the single palladium and the nickel alloys. These have been plotted as though the effective valency of either additive was zero, that is, as if the d bands of the added nickel and palladium were completely filled. If this were true, and if the rigid-band model still applied, the points for these alloys should lie around the heavy broken lines on the plots. In fact, the single palladium alloy gave results which (taken at their face value) indicate no change in the FS, and the nickel alloys show some intermediate behavior. The palladium results are not sufficiently conclusive to merit any serious study. It was found to be extremely difficult to grow a single crystal containing any higher concentration of palladium. The nickel results are of some interest in view of the considerable uncertainty that exists about the precise electronic state of nickel alloyed into copper.

In 1952 Coles²² reviewed the situation and said "all the physical properties . . . indicate the presence of d -band holes in copper-rich copper-nickel alloys, even at nickel contents as low as 5%." Azaroff and Das²³ have reported x-ray absorption spectra which indicate the presence of transitions from the $3d^9$ level of nickel in alloys of copper concentration higher than 60 at.%. Several papers have suggested some form of ferromagnetic interaction or clustering—Shröder²⁴ from electronic specific-heat measurements, van Elst *et al.*²⁵ from magnetization measurements, and Ryan *et al.*²⁶ from magnetic-susceptibility measurements, but the alloys studied contained relatively high concentrations of nickel, that is, $\geq 10\%$. Schroeder *et al.*,²⁷ reporting

²¹ H. C. Yeh and L. V. Azaroff, *J. Appl. Phys.* **38**, 4034 (1967).

²² B. R. Coles, *Proc. Phys. Soc. (London)* **B65**, 221 (1952).

²³ L. V. Azaroff and B. N. Das, *Phys. Rev.* **134**, A747 (1964).

²⁴ K. Shröder, *J. Appl. Phys.* **32**, 880 (1961).

²⁵ H. C. Van Elst, B. Lubach, and G. J. van den Berg, *Physica* **28**, 1297 (1962).

²⁶ F. M. Ryan, E. W. Pugh, and R. Smoluchowski, *Phys. Rev.* **116**, 1106 (1959).

²⁷ P. A. Schroeder, R. Wolf, and J. A. Woollam, *Phys. Rev.* **138**, A105 (1965).

thermoelectric-power measurements, have concluded that they are unable to interpret the results of measurements on dilute copper-nickel alloys in terms of Fermi-surface changes (as they do for silver-palladium) because of their anomalous physical properties.

The most reasonable interpretation of the present results, both in the FS and scattering temperature measurements, seems to lie in Friedel's²⁸ "virtual bound d -level" model. His discussion concludes that nickel (and cobalt) in copper should *not* show any splitting of the virtual bound level such as occurs for iron, manganese, and chromium, but that the d shell should occupy one broad virtual level lying across the Fermi level with room for five electrons of each spin direction, making a total of ten. Our results suggest that roughly 0.4 electrons per atom of nickel are contributed to the conduction band, leaving the other 9.6 electrons in the virtual bound level. This condition is indicated by the lightly dashed line in Fig. 1. The existence of this virtual bound level at the Fermi level will explain the temperature-independent paramagnetism and increased electronic specific heat observed in dilute alloys of nickel in copper. It will also give rise to the relatively large scattering cross section which nickel shows for belly electrons in copper (see below). In support of our interpretation Pelleg²⁹ has shown that an effective valency of about 0.3 for nickel in copper gives good agreement between theory and experiment concerning the activation energy for diffusion of nickel in copper.

It would obviously be valuable to extend the FS studies to higher nickel concentrations, either with a more refined dHvA technique or with some other method such as positron annihilation. A study of the FS changes and scattering effects with impurities which do show the splitting of bound levels would also be of some interest, if only to add to our knowledge of the conditions which give rise to resistance minima and giant thermopowers.

B. Scattering Temperatures

The results of the scattering-temperature measurements for belly and neck oscillations have been plotted in Figs. 3 and 4 against alloy resistivity (actual, or as calculated in the case of zinc), and in Fig. 5 to compare x_N and x_B for the same specimens. Brailsford³⁰ has pointed out that when Dingle¹² discusses the relationship $x = \hbar/\pi k\tau_D$ between an "equivalent temperature" x and a lifetime τ_D , this lifetime is not defined in the conventional way but is equal to *twice* the conventional lifetime τ ; that is, $x = \hbar/2\pi k\tau$. Thus the lifetimes which King-Smith³ and others have derived from dHvA measurements should be *halved* for realistic comparison with τ_p . This is a lifetime derived from resistivity by the relationship $\tau_p = m_B^*/ne^2\rho$, using the simplifying

²⁸ J. Friedel, *Nuovo Cimento Suppl.* **7**, 287 (1958).

²⁹ J. Pelleg, *Phys. Status Solidi* **22**, K83 (1967).

³⁰ A. D. Brailsford, *Phys. Rev.* **149**, 456 (1966).

assumptions of a spherical FS and constant (equal to that for belly electrons) effective mass. From this lifetime one can define an "effective resistivity temperature" $x_p = \hbar/2\pi k\tau_p$. Using a simple scattering potential model, Brailsford shows $\tau/\tau_p \leq 1$, (that is, $x/x_p \geq 1$) with a value of ~ 0.7 (~ 1.4) appropriate to a reasonable form of scattering potential for a charged impurity. Line B in Fig. 3 is equivalent to the lower limit of 1 for x_B/x_p ; in fact, most of our results lie above 1.4. Ziman,³¹ in discussing the anisotropy of relaxation times in the noble metals, has shown that the scattering will vary with the character of the electron wave functions on different parts of the FS. Dugdale and Bailyn,³² in amplifying this discussion, distinguish three types of electron-scattering impurity: (a) the uncharged impurity, whose scattering is strongly localized; (b) the charged impurity; and (c) the transition-metal impurity. We have no example of (a) in the present work. The scattering in this case would be mainly of the *s* electrons on the belly. The ratio x_N/x_B should then be less than unity, but the scattering cross section of this impurity for belly electrons would not be abnormally large. Type (b) is represented by zinc, aluminum, and cadmium in our measurements. Here the scattering of belly *s* electrons and neck *p* electrons should be more or less equal. Ziman³¹ has estimated $x_N/x_B \approx 1.5$ for heterovalent scatterers. Our results show tolerably good agreement with this value (line Z in Fig. 5), but there is clearly a rather strong disagreement between our results and those of Dugdale and Basinski³³ who derive a figure equivalent to $x_N/x_B \approx 0.5$ for heterovalent scatterers from the study of departures from Matthiessen's rule. This disagreement possibly results from the rather sweeping assumptions Dugdale and Basinski had to make in establishing and using their two-band model.

Nickel is presumably representative of type (c) impurities. The localized *d* states discussed above in reference to the FS changes will scatter the *d*-like electrons of the concave parts of the belly (see Dugdale

and Bailyn³²) strongly and thus give rise to the relatively large scattering cross section of nickel in copper (about five times larger than zinc, though still several times smaller than iron or cobalt). This large scattering of the *d*-like belly electrons will result in a small value of x_N/x_B , even though the *s* and *p* scattering is similar to that occurring with the nontransitional heterovalent impurities. Our results, showing that x_N/x_B for the nickel alloys lies significantly below 1.5, lend reasonable support to this interpretation.

We have not yet considered the effect of dislocations. Pippard³⁴ and Chambers³⁵ have shown that dislocation scattering can be particularly severe for neck electrons. Dugdale and Basinski³³ in their Matthiessen's-rule studies have estimated the scattering anisotropy x_N/x_B to be about ten times greater for dislocations than for heterovalent impurities. Some (unpublished) attempts in this laboratory to investigate in a systematic way the effect of dislocation scattering, by measuring dHvA amplitudes in fatigued samples of copper, ran into some difficulties because of the tendency of dislocations to gather into clumps leaving relatively dislocation-free regions which continued to give strong signals. In the present experiments there is no metallurgical reason to expect any *systematic* variation of dislocation density between the various alloys. There will certainly be some *random* variation of dislocation density between specimens which is presumably responsible for some of the observed scatter of data points, particularly those showing anomalously high values of x_N .

ACKNOWLEDGMENTS

The authors are indebted to various past and present, temporary and permanent members of the Solid State Physics group for many useful discussions and for their comments on the paper; in particular, Dr. P. T. Coleridge, Dr. J. S. Dugdale, Dr. J.-P. Jan, and Dr. D. Shoenberg. They also wish to thank A. A. Croxon for invaluable technical assistance and J. W. Fisher for preparing the alloys.

³¹ J. M. Ziman, Phys. Rev. **121**, 1320 (1961).

³² J. S. Dugdale and M. Bailyn, Phys. Rev. **157**, 485 (1967).

³³ J. S. Dugdale and Z. S. Basinski, Phys. Rev. **157**, 552 (1967).

³⁴ A. B. Pippard, Proc. Roy. Soc. (London) **A287**, 165 (1965).

³⁵ R. G. Chambers, Proc. Phys. Soc. (London) **89**, 695 (1966).